ENVIRONMENTAL RESEARCH
LETTERS

LETTER • OPEN ACCESS

Markers of economic activity in satellite aerosol optical depth data

To cite this article: Shobha Kondragunta *et al* 2023 *Environ. Res. Lett.* **18** 084013

View the article online for updates and enhancements.

ENVIRONMENTAL RESEARCH
LETTERS

OPEN ACCESS

RECEIVED
13 April 2023

REVISED
23 June 2023

ACCEPTED FOR PUBLICATION
5 July 2023

PUBLISHED
20 July 2023

LETTER

Markers of economic activity in satellite aerosol optical depth data

Shobha Kondragunta[1,*], Zigang Wei[2], Hai Zhang[2], Hongqing Liu[2], Istvan Laszlo[1], Bin Zhang[3], Changyong Cao[1] and Pubu Ciren[2]

[1] NOAA NESDIS 5825 University Research Court, College Park, MD, United States of America
[2] IM Systems Group 5830 University Research Court, College Park, MD, United States of America
[3] University of Maryland at College Park, 5825 University Research Court, College Park, MD, United States of America
[*] Author to whom any correspondence should be addressed.

E-mail: Shobha.Kondragunta@noaa.gov

Keywords: aerosol optical depth, nitrogen dioxide, emissions, particulate pollution

Supplementary material for this article is available online

Abstract

This study investigated the impact of COVID-19 lockdowns on satellite aerosol optical depth (AOD), to explore the hypothesis that if changes in economic activity are seen in emissions of NO_2, an aerosol precursor, then AOD should change commensurably. We developed a technique to filter AOD data to isolate changes associated with anthropogenic emissions. Overall, in 37 of the 43 cities that were identified as top oxides of nitrogen (NO_x) emitters from their transportation sectors, AODs decreased by 21.2% ± 7.8%, 18.9% ± 11.7%, 27% ± 12.4%, 22.9% ± 7.6% in the United States, India, western Europe, and China, respectively—an average of 22.4% ± 7.4%. In contrast, AODs increased on average by 11.7% ± 8.4% in Taiwan, where economic stimulus was used as a strategy during the pandemic. This analysis implies NO_x and volatile organic compounds emissions reductions from the transportation sector can be targeted, and by transitioning 6 million light duty vehicles from gasoline to electricity, the US can achieve 21% improvement in AOD.

1. Introduction

The impact of sudden/short-term economic activity changes on anthropogenic emissions and associated air pollution during the shutdown of traffic during major public events such as the 2008 Beijing Olympics has been reported by many studies (Cermak and Knuff 2009, Tan *et al* 2009, Witte *et al* 2009, Wang *et al* 2010, 2017, 2021, Hao *et al* 2011, Guo *et al* 2013, Ding *et al* 2015, Sun *et al* 2016, Tong *et al* 2016, Zhao *et al* 2017, Li *et al* 2019). Some of these studies used satellite observations of Ozone Monitoring Instrument (OMI) tropospheric column nitrogen dioxide (tropNO_2). As reported by the meta-analysis of Gkatzelis *et al* (2021) more recently, Tropospheric Monitoring Instrument (TROPOMI) tropNO_2 data were used to document the impact of COVID-19 pandemic related lockdown on its changes and attributed those reductions to improvements in air quality in general. Though NO_2 by itself is a harmful pollutant that leads to human health impacts, its role in the photochemical production of ozone and fine particulate matter (particles $< 2.5\ \mu$m, $PM_{2.5}$) is the most important as these are the two pollutants with harmful human health impacts that are monitored at the surface to determine if air quality is good or bad. In countries like the US, the national NO_2 standard is weak and no location is out of compliance (Kroll *et al* 2020). Ozone and $PM_{2.5}$ are photochemically formed from precursor gaseous pollutants that include nitrogen oxide and nitrogen dioxide ($NO + NO_2 = NO_x$), sulfur dioxide (SO_2), ammonia (NH_3), and volatile organic compounds (VOCs), hereafter referred to simply as precursor gaseous emissions (Kroll *et al* 2020).

$PM_{2.5}$ is harmful to human health and is regulated across the globe. While particles are directly emitted into the atmosphere from the use of fossil fuels, they are also photochemically produced by oxidation of precursor gaseous emissions. Particle concentrations can be directly measured or inferred from optical measurements (column integrated light extinction in unitless quantity called aerosol optical depth, AOD) due to their absorption and scattering properties.

Therefore, any changes in economic activity that lead to changes in primary and precursor emissions could lead to associated changes in AOD.

This study investigated the impact of COVID-19 lockdowns on satellite AOD, to explore the hypothesis that if changes in economic activity are seen in emissions of NO_2, an aerosol precursor, then AOD should change commensurably. It is shown that during the COVID-19 lockdowns in the US, when human activity decreased, NO_x emissions from traffic (passenger vehicles) dropped dramatically (Kondragunta *et al* 2021). Carbon monoxide, VOCs and NO_x are the dominant emissions from vehicular (cars and trucks) combustion exhaust in addition to greenhouse gases, but of these, VOCs and NO_x lead to secondary ozone and $PM_{2.5}$ formation. Primary $PM_{2.5}$ emissions are fifty times lower than NO_x emissions from cars and trucks according to the Environmental Protection Agency emissions inventories in the US and thus are not a significant source for AOD (www.bts.gov/content/estimated-national-average-vehicle-emissions-rates-vehicle-vehicle-type-using-gasoline-and).

Reductions in emissions of precursor gases and $PM_{2.5}$ from traffic and industrial sources led to low aerosol concentrations and thus low AODs during the COVID-19 pandemic related lockdowns (Kumar *et al* 2020, Kumari *et al* 2020, Venter *et al* 2020, Zheng *et al* 2020, Hammer *et al* 2021, Khan *et al* 2021, Straka III *et al* 2021). Studies that investigated the impact of reduced emissions on climate found that though AOD decreased, the decrease was not large enough to detect changes in clouds, radiation, surface temperature etc. due to natural variability (Gettelman *et al* 2021, Jones *et al* 2021). Interpreting changes in $PM_{2.5}$ is complicated due to complex photochemistry related to secondary aerosol formation as well as emissions of primary particulates from natural and anthropogenic sources (Kroll *et al* 2020, Venter *et al* 2020, Hammer *et al* 2021). Even though Hammer *et al* (2021) used a global chemistry and transport model to separate the effects of meteorology and assumed transportation sector emissions changes of 50% due to lockdowns on $PM_{2.5}$, they did not include the contributions of smoke from fires and the differences in fire activity between 2020 and 2019. Additionally, Hammer *et al* (2021) did not trace the exact reduction in secondary aerosol formation due to reduction in NO_x emissions compared to the reduction in primary particulate emissions. Similarly, Venter *et al* (2020) attributed observed $PM_{2.5}$ increases in 2020, despite the lockdowns, to transported aerosol and cited historical burning patterns in areas where $PM_{2.5}$ increases were observed. In addition to weather, variability in emissions from natural sources and the long-term trends in $PM_{2.5}$ must be considered when assessing the impact of lockdowns on $PM_{2.5}$ and AOD.

Indeed, in many parts of urban areas dominated by NO_x and VOC emissions from the transportation and industrial sectors, interpreting changes in $PM_{2.5}$ or AOD can be difficult due to regional transport of smoke or dust impacting local air quality. Additionally, the true change in AOD due to emissions changes in 2020 can only be identified after removing the long-term trend in AOD due to various clean air emissions controls in place across the world, especially in China as reported by Sogacheva *et al* (2018).

The main focus of this study is to develop a method to use satellite data to detect AOD changes due to changes in anthropogenic NO_x emissions when there are changes in economic activity that last for a month or longer using the impacts of COVID-19 lockdowns on AOD as a case study. We used Suomi National Polar-orbiting Partnership satellite Visible Infrared Imaging Radiometer Suite (Suomi NPP VIIRS) AOD retrievals, along with Sentinel-5 Precursor satellite TROPOMI tropNO$_2$ observations as markers for urban/industrial pollution to isolate the impact of anthropogenic emissions changes on AOD. In this study, SO_2 emissions were not a focus because traffic emissions are not a significant source for SO_2 (McDuffie *et al* 2020). Globally, SO_2 emissions have fallen by 32% between 2004 and 2017 primarily due to the implementation of stricter emission standards for the energy and industry sectors after 2010 in China (Zheng *et al* 2018).

2. Materials and methods

2.1. Suomi NPP VIIRS AOD

The Suomi NPP satellite VIIRS has been providing a pixel-level (~750 m) AOD product for various user applications (e.g., Huff *et al* 2021, Li *et al* 2021, Zhang and Kondragunta 2021). In order to put into perspective, the observed VIIRS AOD changes due to changes in economic activity measures, we wanted to ensure that the AOD record is consistent and devoid of any artificial trends. Therefore, we reprocessed 9 years of VIIRS AOD with an improved sensor calibration as well as an enhanced algorithm that provides retrievals over both dark vegetated and bright surfaces (Laszlo and Liu 2016, Zhang *et al* 2016, Laszlo 2018). The recalibrated radiance data have improved long-term stability (better than 0.3%) and accuracy with uncertainty < 2% (Uprety *et al* 2020, Cao *et al* 2021). It also incorporated a bias correction for the reflective solar bands, which addressed known calibration biases for VIIRS bands M5 (0.672 nm) and M7 (0.865 nm). Other improvements to the calibration included terrain correction, straylight correction, and corrections to anomalies in the thermal bands. The reprocessed VIIRS AODs were compared to a global network of ground-based Sun photometers using match-up criteria defined by Liu *et al* (2014).

For the validation of the reprocessed AOD data, we stratified the AODs into three categories: AODs lower than 0.1, between 0.1 and 0.8, and greater than 0.8. For these three AOD ranges, the global mean biases/root mean square errors were found to be 0.02/0.048, 0.008/0.06, and −0.121/0.39, respectively.

2.2. Sentinel-5 Precursor TROPOMI tropospheric NO_2

The Sentinel-5 Precursor satellite, containing the TROPOMI sensor, orbits the Earth in formation with Suomi NPP, and as a result, VIIRS AOD and TROPOMI tropNO_2 are considered observations of the same atmospheric column. The NO_2 algorithm retrieves total column NO_2 and separates the stratosphere from troposphere using the chemical transport model predicted stratospheric NO_2 analysis fields (van Geffen *et al* 2019). TROPOMI's tropNO_2 product (3.5 km × 5.6 km) with retrieval quality flag greater than 0.75 is used in this study.

Sources of error (∼25%) in tropNO_2 include altitude dependent air mass factors, stratosphere-troposphere separation of NO_2, a priori NO_2 profile and shape, surface albedo climatology, and calibration errors as a function of view angle (van Geffen *et al* 2019, Chan *et al* 2020, Ialongo *et al* 2020, Judd *et al* 2020, Zhao *et al* 2020).

2.3. NO_2 filter for AOD (NO_2F4AOD) to screen non-anthropogenic sources of aerosols

We developed a method to screen VIIRS AOD data using tropNO_2 data to isolate changes in AOD associated with changes in anthropogenic emissions. The rationale we took to develop this method is that NO_2 is short-lived and observed near source regions whereas aerosols have a longer lifetime and can be transported long distances. For example, emissions of NO_x from fires are 8.3 times lower than $PM_{2.5}$ (Andraea 2019). Accordingly, when a transported smoke plume reaches an urban/industrial area, tropNO_2 concentrations are small but AOD values are high (Veefkind *et al* 2011). Given this scenario, when anthropogenic sources are dominant, both NO_2 and AOD values are elevated but when biomass burning sources are dominant, AOD values are higher and NO_2 values are lower.

In this NO_2F4AOD method, we looked at tropNO_2 and AOD changes to see if they co-increased or co-decreased between 2020 and 2019 and filtered AOD data based on absolute changes in tropNO_2 greater than 8 μmoles m^{-2}, which is the expected retrieval error (van Geffen *et al* 2019). The NO_2F4AOD method shown in figure 1 illustrates how the filtering of AOD is carried out. The top left panel shows the mean AOD difference between 2020 and 2019 for 10 February to 25 February. This period corresponds to the first COVID lockdown in China. AODs decreased in the central part of China corresponding to Hubei province, but there are increases in AODs in the southwestern and northeastern part of China; many studies reported similar findings indicating that warm and humid conditions were favorable for the production of sulfate aerosol from SO_2 emissions in northeastern China (Le *et al* 2020, Anderson *et al* 2021, Loeb *et al* 2021, Kong *et al* 2023). The tropNO_2 image for the same period, in the bottom left panel, shows a decrease in tropNO_2 in the same regions where AOD decreased, but no noticeable or significant tropNO_2 increases corresponding to the increase in AODs in southwestern and northeastern China are present.

Prior to applying our screening method, we calculated background rural tropNO_2 using TROPOMI data and found it to be ∼16 μmoles m^{-2} (Kondragunta *et al* 2021); this background value was subtracted from daily TROPOMI tropNO_2 data to isolate clusters of elevated tropNO_2 values associated with urban/industrial sources. Once we pass the AOD data through the filter (background tropNO_2 > 16 μmoles m^{-2} and ΔtropNO_2 > 8 μmoles m^{-2}, ΔAOD co-increase or co-decrease along with ΔtropNO_2), the AOD increases in southwestern China disappear, but some increase in AOD remains in northeastern China. Similarly, the increases in AOD over the ocean also disappear after application of the filter.

The differences in tropNO_2 and in AOD between 2020 and 2019 due to meteorology were minimized by averaging the satellite data for the duration of the lockdown period (approximately a month or longer). When looking for signatures of emissions changes in satellite observations between different years, averaging the data over 30 d is expected to minimize the influence of meteorology and differences in sampling in satellite data due to clouds (Kondragunta *et al* 2021, Liu *et al* 2021). However, the influence of meteorology can remain especially when change in NO_x emissions is small (Wang *et al* 2021). This technique was applied to track changes in AOD between 2020 and 2019, in order to see the magnitude of changes in AOD, but ideally a reference climatology should be used because of interannual variability in meteorology that is not fully accounted for when differences between 2 years are used. The NO_2F4AOD method could not be applied over longer time periods because tropNO_2 data are available only from 2018. To circumvent this problem, we identified the top 5% NO_x emitting urban/industrial regions from the 2019 Community Emissions Data System (CEDS) emissions inventory and conducted an AOD time series analysis to account for the long-term trend present in AOD observations. Instead of using the traditional least-squares fit analysis to identify the long-term trend in the AOD time series data, we used the Theil-Sen slope method and determined the significance of the derived trends using the Mann–Kendall test (Thiel 1950, Sen 1968). This method is insensitive to outliers and is shown to be significantly more

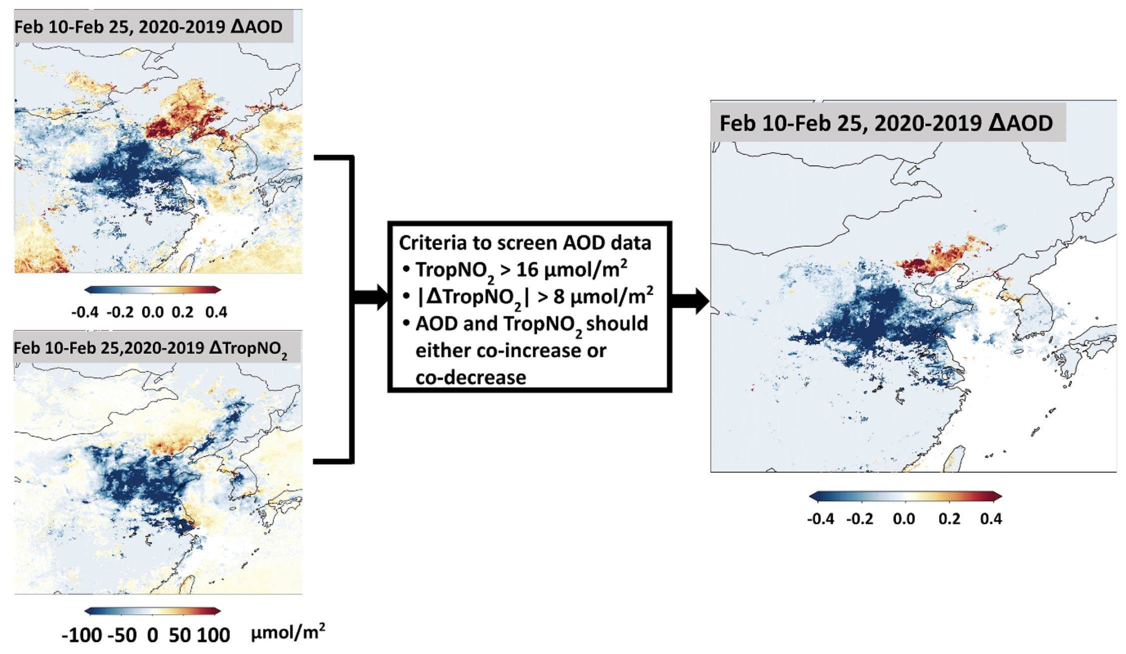

Figure 1. Schematic of method to filter AOD data using tropNO$_2$.

accurate than the least squares method. We also confirmed that these top 5% NO$_x$ emitting urban/industrial regions are under the influence of high NO$_x$ emissions from the transportation sector by analyzing the 2019 CEDS (McDuffie *et al* 2020). Finally, in reporting AOD changes due to the COVID lockdowns in various cities across the globe in 2020 compared to climatology, we accounted for the long-term AOD trend by adding the trend value to 2020 AODs.

3. Results

Figure 2 shows VIIRS AOD changes ($\Delta AOD_{2020-2019}$) identified due to changes in emissions between 2020 and 2019 for China, India, western Europe, and the US. The panels in the left column (figures 2(a)–(d)) are unfiltered data, whereas the panels in the right column (figures 2(e)–(h)) are filtered using NO$_2$F4AOD. The 2020 lockdown periods are different for these four regions: China from 23 January to 8 April, Europe from 9 March to 4 July, US from 19 March to 15 April, and India from 25 May to 7 June.

Of the four regions investigated, the unfiltered VIIRS AOD changes in every region showed a combination of decreases (areas in blue) and increases (areas in red) during the lockdowns. However, the $\Delta AOD_{2020-2019}$ from the NO$_2$F4AOD method removed the increases associated with non-anthropogenic sources (e.g., smoke from fires, blowing dust). The largest reductions in AOD were observed in China because that is where AOD levels associated with urban/industrial pollution are the highest in the globe. Figure S1 shows 2019 annual mean AOD for US and China showing that pollution in China is four times greater than in the US. The lockdown areas of Hubei province, which includes Wuhan and other cities, resulted in an $\Delta AOD_{2020-2019}$ change up to 0.2 over 2 months, but during the most stringent portion of the lockdown, from 10 February to 25 February, the $\Delta AOD_{2020-2019}$ values decreased by up to 0.5. For a typical AOD value of unity corresponding to pollution, this is a 50% decrease.

There are some areas in China with increases in $\Delta AOD_{2020-2019}$ due to smoke from fires; analysis of Suomi NPP VIIRS fire detection and fire radiative power (FRP) products shows distinct correlation with elevated levels of fire intensity in areas where an increase in $\Delta AOD_{2020-2019}$ was observed. Figure S2 shows the difference in VIIRS smoke fraction between 2020 and 2019 in Asia. Fires in some regions in 2020 were quite strong, and smoke from these fires offset the reductions in AODs from lockdowns, especially in urban areas closer to the fires. Though Chinese cities such as Chengdu, Chongqing, Guiyang, Kunming, and Nanning are among the top 5% NO$_x$ emitting cities, $\Delta AOD_{2020-2019}$ values increased in these cities because they were under the influence of locally transported smoke due to their proximity to intense burning in Southeast Asia. These local/regional transport of smoke from fires is a well understood phenomenon (Zhu *et al* 2017, 2022). Note that over long distances, tropNO$_2$ from fires is not detected, but over short distances, it is still observed in smoke plumes; distance traveled by smoke plumes depends on wind speed and varies from one fire event to another. These increases are not due to unaccounted meteorological differences between 2020 and 2019 in our analysis; consistent with our analysis, Hammer *et al* (2021) showed no such AOD increases due to meteorology in their model simulations. The increase in $\Delta AOD_{2020-2019}$

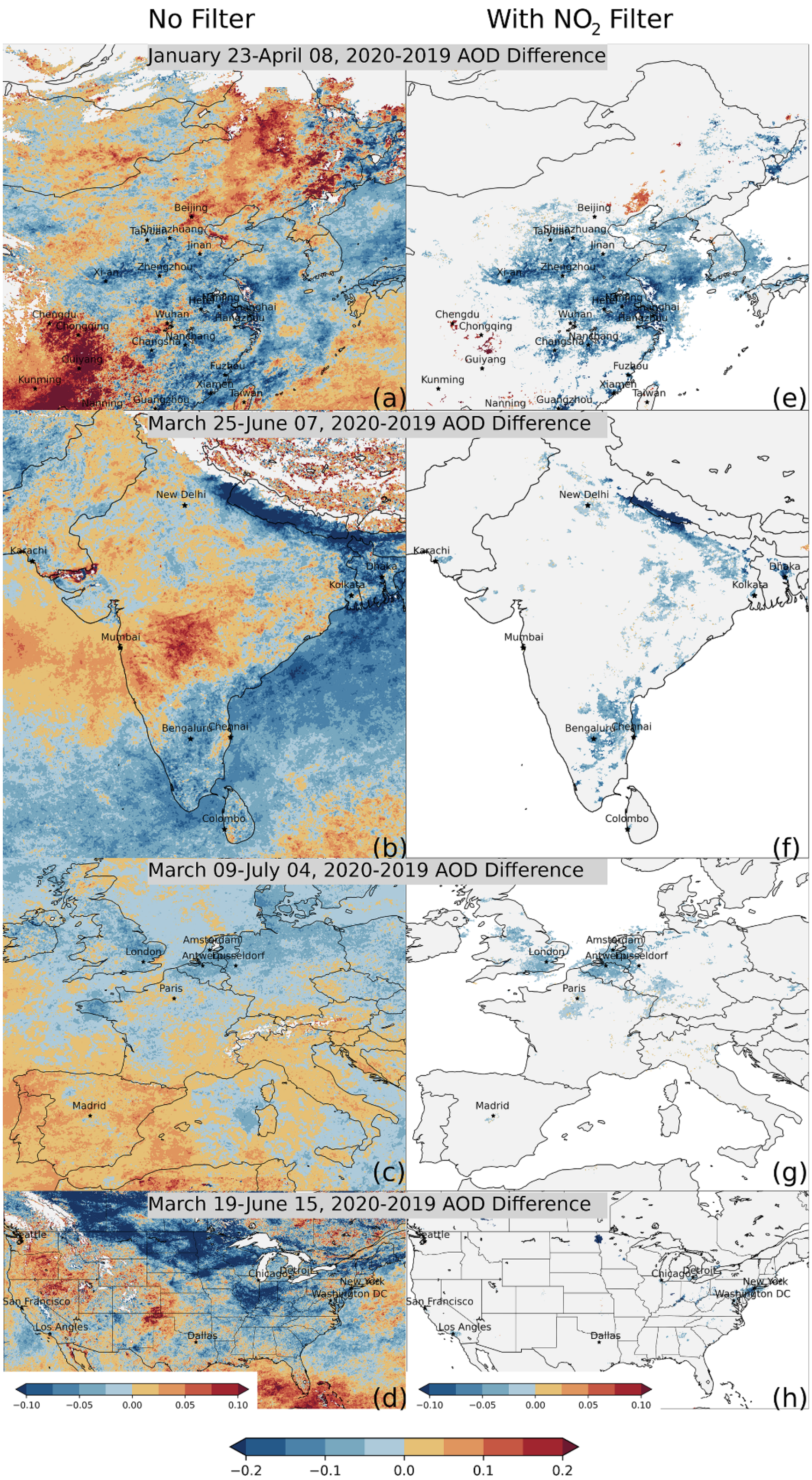

Figure 2. VIIRS AOD changes ($\Delta AOD_{2020–2019}$) identified due to changes in emissions between 2020 and 2019 for China (a), India (b), western Europe (c), and the United States (d) without any filter. $\Delta AOD_{2020–2019}$ for China (e), India (f), western Europe (g), and the United States (h) with NO_2F4AOD screening. Note color bar for (d) and (h) is from −0.1 to 0.1.

northeast of Beijing, however, does not correspond to an increase in fire activity between the 2 years. Other studies that performed model simulations attributed the increase in $\Delta AOD_{2020–2019}$ in that region to sulfate and organic aerosols from energy and industrial sectors (Miyazaki *et al* 2020, Hammer *et al* 2021). Studies have also shown that warm and humid conditions and shallow boundary layer enhanced sulfate aerosol production in 2020 compared to 2019 (Le *et al* 2020, Su *et al* 2020, Andersen *et al* 2021, Loeb *et al*

2021). Additionally, in downwind regions of China such as Seto Island Sea, AOD changes were minimal because SO_2 emissions from ships that are a source of sulfate aerosol along with industrial emissions did not change much between 2020 and 2019 though they have been trending downward (Itahashi *et al* 2021).

In India, emissions from the transportation sector, power plants, and industry dropped by up to 75% during the lockdown (Tibrewal and Venkataraman 2022). This led to lower values of AOD as observed by satellite data; in the unfiltered AOD map (figure 2(b)), the entire Indo-Gangetic plain and southern India showed reductions in AOD, whereas central India showed increases in AODs. The increase in $\Delta AOD_{2020–2019}$ in central India is attributed to intense fires in 2020 compared to 2019 (figure S2); AOD filtered using NO_2F4AOD shows only decreases in AOD (figure 2(f)). Mishra and Rathore (2021) reported a 30% increase in fire activity in India in 2020 compared to 2019, which is consistent with the VIIRS smoke fraction difference between 2020 and 2019 shown in figure S2. It is notable though that the smoke fraction was higher in 2020 compared to 2019 in most parts of India including the Indo-Gangetic plain region. Despite the increased fire activity in 2020, AODs decreased overall during the lockdown. This is either due to this region being dominated by anthropogenic sources that lead to very high AODs and may even be higher or comparable to AODs due to smoke from fires or unusually high precipitation observed in 2020 (Sathe *et al* 2021).

In Europe, emissions from the transportation sector decreased by 89% (Spain), 86% (Italy), 82% (France), 47% (Germany), and 70% (United Kingdom) during the lockdowns (Acharya *et al* 2021). Similar to China and India, domestic energy consumption in Europe increased due to work-from-home activities yet reductions in retail and recreation activities led to $\Delta AOD_{2020–2019}$ decreases.

In the US, after filtering for AOD changes not associated with the lockdown, small decreases in AOD were observed in the Interstate-95 corridor in the Northeast US (major transportation pathway), Los Angeles, San Francisco, and the Southeast US. The increased AODs over the Gulf of Mexico in the unfiltered data (figure 2(d)) are due to the month-long Saharan dust transport event that occurred in June 2020 (Asutosh *et al* 2022); our NO_2F4AOD filtered out those high AODs (figure 2(h)). Our findings for AOD changes in the US are consistent with Hammer *et al* (2021), Naeger and Murphy (2020), and Acharya *et al* (2021). Analysis of NOAA fuel-based emissions estimates shows that on-road $PM_{2.5}$ emissions decreased by 40% in Los Angeles and 55% in New York compared to a pre-COVID scenario. These reductions in emissions during the lockdown period are substantial but the magnitude of primary $PM_{2.5}$ emissions is small; decreases in AOD are the benefit of reductions in NO_x and VOC emissions. Acharya *et al* (2021) report that some of the $\Delta AOD_{2020–2019}$ increases seen in the US are attributable to a 30% increase in SO_2 emissions combined with high relative humidity and low wind speed that led to secondary sulfate aerosol formation. These increased AODs are filtered out in our analysis as we screen AOD using the tropNO_2 filter and SO_2 emissions are negligible from the transportation sector.

To quantify the changes in $\Delta AOD_{2020–2019}$ in major urban/industrial regions dominated by emissions from the transportation sector, we identified 43 cities encompassing the top 5% NO_x emitting regions across the globe and calculated the percent change in AOD (figures 3(a), (c), (e) and (g)). Barring cities such as Chengdu, Chongqing, Guiyang, and Nanning that were under the influence of smoke transport, most regions in China showed an overall AOD decrease of 22.9%± 7.6%. Similarly, $\Delta AOD_{2020–2019}$ decreased by 21.2%± 7.8% in the US, 27%± 12.4% in Europe, 18.9%± 11.7% in India.

In figures 3(b), (d), (f) and (h), we show analysis of AOD changes in the 43 cities using climatology as a reference. Instead of comparing tropNO_2 filtered AOD data between 2020 and 2019, we used AOD data from 2012 to 2019 to conduct a time series analysis using the Theil-Sen method (Theil 1950, Sen 1968). This method accounts for the long-term trend in AOD and isolates AOD changes strictly due to lockdown-related emissions changes. The results are consistent with those obtained from the NO_2F4AOD method (figures 3(a), (c), (e) and (g)). Mean AOD decrease, including cities that showed AOD increases using NO_2F4AOD method is 16.5% and with the analysis using climatology as a reference, the mean AOD decrease is 18.5%.

The impact of the lockdowns on AOD changes was found to be marginally sensitive to the way the analysis is carried out, especially for cities that were in close proximity to fire activity. When considering the cities in the analyses reported in figure 3, we used the city perimeter based on population density polygons. For cities in the US, the metro area polygons were taken from the 1:500 K TIGER line/shape files downloaded from www.census.gov/geographies/mapping-files/time-series/geo/tiger-line-file.2019.html. For other countries, the city polygons were downloaded from https://gadm.org/data.html. The Global Administrative Areas (GADM) are free licensed worldwide high-resolution data available to the public. In our analysis, for most cities, we used administrative level 2 data or manually combined a group of nearby level 2 and level 3 cities.

We also did another set of analyses where we identified the city center and used a radius of 27.5 km to

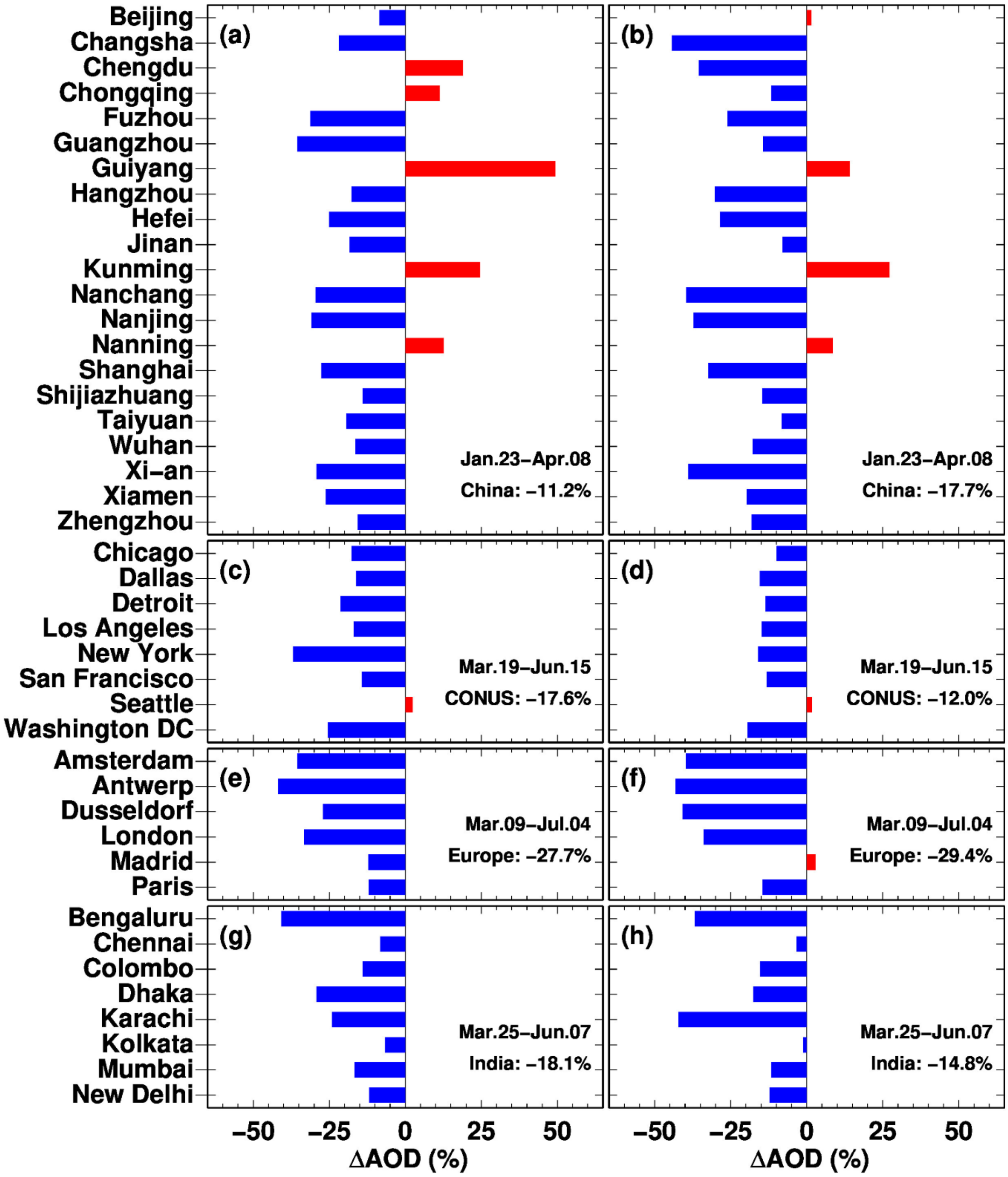

Figure 3. Impact of COVID lockdowns on AOD estimated from NO_2F4AOD method for different cities in (a) China, (c) Contiguous United States, (e) Europe, and (g) India. Cities highlighted in red are regions where AOD increased due to transported smoke, except in Taiwan where lockdowns were not imposed. (b), (d), (f) and (h) are estimates for the same cities and regions using Thiel–Sen slope method.

define the heart of the city. The results are consistent for most cities in magnitude and sign of AOD change. However, for Nanning, Guiyang, Beijing, and Kunming in China, we found major differences and attribute them to these regions being under the influence of smoke from nearby fires (table 1). For Nanning and Guiyang, the sign of AOD change did not flip but the magnitude of the impact was found to be greater when polygon shape was used to identify the city. For Beijing, when non-polygon shape was used to identify the city, there was no AOD change but when polygon shape was used, the AOD change was −8%. For Kunming, there was no AOD change using non-polygon shape, but the AOD change was 50% using polygon shape. This is expected because Kunming was under heavy influence of smoke and the wider the spatial area considered, the larger the influence of smoke from fires. For all other cities in Europe, India, and the US, no major differences were found in the AOD changes based on the two estimates.

The robustness of our AOD changes due to lockdowns were also cross-verified using Synthetic Control Methods (Abadie 2021). Using this method, we investigated AOD changes in Wuhan, Beijing, and Shanghai in China. In this purely statistical approach, we tested the effect of intervention (lockdown) by

Table 1. $\Delta AOD_{2020–2019}$ for 43 cities across the globe with two different spatial averaging methods.

China			India			Europe			USA		
City	Non-polygon city shape (%)	Polygon city shape (%)	City	Non-polygon city shape (%)	Polygon city shape (%)	City	Non-polygon city shape (%)	Polygon city shape (%)	City	Non-polygon city shape (%)	Polygon city shape (%)
Shijiazhung	−9	−12	New Delhi	−10	−11	Amsterdam	−21	−26	New York	−32	−26
Xi-an	−22	−22	Dhaka	−20	−22	Paris	−9	−11	Chicago	−22	−15
Hangzhou	−11	−15	Karachi	−13	−20	Antwerp	−29	−29	Los Angles	−13	−15
Changsha	−18	−18	Colombo	−19	−13	London	−30	−25	Dallas	−15	−14
Hafei	−17	−20	Bengaluru	−30	−29	Madrid	−11	−12	Detroit	−19	−19
Nanjing	−21	−24	Kolkata	−12	−6	Dusseldorf	−25	−11	Seattle	−8	3
Zhengzhou	−12	−14	Chennai	−18	−14				San Francisco	−11	−14
Chongqing	12	13	Mumbai	−3	−8				Washington, DC	−21	−19
Xiamen	−23	−21									
Taiyuan	−11	−16									
Nanchang	−21	−23									
Jinan	−11	−15									
Wuhan	−9	−14									
Shanghai	−18	−22									
Chengdu	25	23									
Fuzhou	−23	−25									
Nanning	8	18									
Guangzhou	−20	−26									
Guiyang	47	62									
Beijing	0	−8									
Kunming	0	50									

constructing a weighted combination of controls from similar cities outside of China that did not have lockdowns at the same time. Based on this analysis, AOD changes in 2020 due to the lockdown in Wuhan, Beijing, and Shanghai were −18.1%, 13%, and −12%. Though AODs decreased in 2020 for Wuhan and Shanghai, the magnitude (−12%) is smaller than the value estimated from the $tropNO_2$ filter method (−21%) and the Thiel–Sen slope method (−23%). For Beijing, the AOD change estimated using SCM is consistent with the other two methods.

To test if our methods work for the opposite scenario where economic activity increases, we applied our methods to Taiwan, which did not use lockdowns to curb the spread of the COVID-19 pandemic but instead used isolation from the rest of the world. During the pandemic, Taiwan invested nearly one trillion Taiwanese Dollars ($T) into its economy, which grew by 2% in the first quarter, and due to which its exports to China increased by 10.3% in May 2020 compared to May 2019 (www.brookings.edu/blog/order-from-chaos/2020/06/29/taiwan-faces-a-changed-economic-outlook-in-asia-following-covid-19/). When AODs in the northern, central, and southern Taiwan regions were analyzed using NO_2F4AOD method, we found that AODs in 2020 increased by 1.5%, 11.4%, and 12.1% for northern, central, and southern Taiwan respectively. The AOD changes estimated from the Thiel–Sen slope method also showed increased AODs but slightly smaller in magnitude: 1.5%, 2.3%, and 7.9% for northern, central, and southern Taiwan respectively. Figure S3 shows $\Delta AOD_{2020–2019}$ for Taiwan for February with and without NO2F4AOD method that shows how AODs increased in 2020 due to economic activity stimulated by new investments.

The premise of this study is based on the assumption that $tropNO_2$ and AOD co-vary in polluted regions across the globe. This assumption has been tested two different ways. First, by analyzing relationship between $tropNO_2$ and AOD for 2019 and 2020 for 43 cities when pandemic related lockdowns were not a factor. Figure S4 shows that our assumptions hold with the relationship between $tropNO_2$ and AOD having a positive linear correlation with a smaller slope when airmasses are dominated by urban pollution whereas when smoke plumes are present, the linear relationship has a much steeper slope. Second, by showing a map of how $tropNO_2$ and AOD co-vary across China between 2020 and 2019 for 10 February to 25 February (figure S5). The $tropNO_2$ and AOD variability is consistent with known knowledge of regions with reduced NO_x emissions from transportation sector. Similarly, we found the regions where AOD increased and $tropNO_2$ decreased to be those influenced by smoke from fires.

Because transportation sector emissions were the most impacted during the lockdowns across the globe, this analysis demonstrates that targeted lowering of NO_x emissions could have a benefit on lowering particulate pollution in favorable meteorological conditions. This can potentially be achieved by transitioning gasoline-based vehicles to electricity, for example. Using the $tropNO_2$ to on-road NO_x emissions relationship ($\Delta tropNO2 = 0.33^{*}\Delta NO_x + 2.33$) and the AOD to $tropNO_2$ ($AOD = 0.0022^{*}tropNO_2 + 0.102$) relationship for the Los Angeles area reported in Kondragunta *et al* (2021), we estimate that 12 million gasoline-based vehicles must be removed from the road on any given day to see the 21% improvement in AOD that was observed across the US during the lockdown. This analysis did not include VOC emissions reductions because we do not have data on the relationship between VOCs and AOD. However, the contribution of NO_x and VOC emissions to $PM_{2.5}$ is 1:1.1 according to the EPA (www3.epa.gov/ttnchie1/conference/ei13/mobile/hodan.pdf). Considering a targeted NO_x and VOC emissions reductions from light duty vehicles, the number of vehicles that need to transition to electricity comes down to 6 million. There are currently only 2.6 million electric vehicles in the US compared to 109 million gasoline powered cars (www.anl.gov/esia/light-duty-electric-drive-vehicles-monthly-sales-updates; dot.gov) that emit ~486 tons of NO_x per day. Transitioning to electric vehicles to reduce particulate pollution appears to be a lofty target because despite the rise in electric car sales, the transition is not fast enough, and it is uneven across the US, with some states doing better than others in electric car sales (https://afdc.energy.gov/data/10962). Emissions of NO_x from gasoline powered light duty vehicles (cars) are the lowest (~0.157 g/mile) whereas diesel powered heavy duty vehicles' NO_x emissions are the highest (~3.518 g/mile). Targeting the transition of diesel operated vehicles to bio-diesel or electricity could be a better policy for effective particulate pollution reductions in the urban areas.

4. Conclusions

The COVID-19 pandemic provided an opportunity for the scientific community to study the influence of changes in economic activity on anthropogenic emissions that lead to harmful pollution and to determine if those changes can be detected in satellite data. In this study, we specifically focused on capturing changes in AOD using satellite data on monthly time scales. To account for AOD data that are influenced by non-anthropogenic sources such as biomass burning, we developed a NO_2F4AOD technique. Using tropNO_2 data to filter AOD data, we isolated the changes in AOD due to changes in reduced emissions from the transportation sector caused by COVID-19 pandemic related lockdowns; overall, in 37 of the 43 cities that were identified as top NO_x emitters from the transportation sector, AODs decreased by 21.2% ± 7.8%, 18.9% ± 11.7%, 27% ± 12.4%, 22.9% ± 7.6% in the United States (7 cities), India (8 cities), western Europe (6 cities), and China (16 cities), respectively—a mean decrease of 22.4% ± 9.4%; when the six cities with increased AOD are included, the mean decrease is 16.5%. These results are consistent with our hypothesis that when tropNO_2 decreases AOD decreases and vice versa except when gains of improved air quality due to reduced NO_x emissions were offset by emissions of aerosols and aerosol precursors from fires; in cities such as Nanning, Guiyang, and Kunming in China that were downwind of major fires; transported smoke increased AODs by up to 23%.

The magnitude of AOD changes were found to be minimally sensitive to the spatial averaging domain or the reference data used. When AOD in 2020 was compared to reference climatology using time series analysis, the mean AOD decrease is found to be 18%, which is similar to the 22% decrease found using NO_2F4AOD method.

Our findings are consistent with many other studies that either analyzed surface $PM_{2.5}$ or AOD data to understand the impact of lockdown on particulate pollution. Specifically, Hammer *et al* (2021) used global model simulations to study the same geographic regions that we studied. Unlike tropNO_2 that is easy to observe in urban/industrial areas near source regions due to the short lifetime of NO_2, aerosols are long-lived and are transported long distances. Therefore, any analysis of AOD data should account for contributions from non-anthropogenic sources such as dust and smoke. Using the species-to-species relationship between tropNO_2 and AOD, we were able to isolate true AOD changes due to lockdowns except in cities that were in close proximity to fires.

We demonstrated that the methods we developed are robust and have the capability to detect and track changes in AOD due to changes in economic activity. When we applied our NO_2F4AOD filtering technique to study AOD changes in Taiwan, we observed a mean 11.7% ± 8.4% increase in AOD across northern, western, southern Taiwan where most of its population and economic activity are concentrated; these AOD increases were expected based on Taiwan's strategy of using economic stimulus and not a lockdown during the COVID-19 pandemic. Going forward, our methods can be successfully applied to track economic changes on aerosols, on global to regional scales, such as power grid and roadway shutdowns associated with hazardous weather conditions (e.g., hurricanes, ice storms, etc). Analysis of these current and past events will provide insights into how effective pollution control strategies can be developed. It is estimated that reducing 6 million light duty vehicles from the US roadways can lead to 21% improvement in particulate pollution.

Data availability statement

The data that support the findings of this study are openly available at the following URL/DOI: http://noaa-jpss.s3.amazonaws.com/index.html#SNPP/VIIRS/SNPP_VIIRS_Aerosol_Optical_Depth_EDR_Reprocessed/.

Acknowledgments

Authors thank Amy Huff (IM Systems Group) for helping with editorial work of the manuscript. Authors thank NOAA's Joint Polar Satellite System program for providing funding to reprocess Suomi NPP VIIRS AOD data.

Discalimer

The scientific results and conclusions, as well as any views or opinions expressed herein, are those of the author(s) and do not necessarily reflect those of NOAA or the Department of Commerce.

Open research

The reprocessed Suomi NPP VIIRS AOD data at native pixel-level as individual 86 s granules can be obtained from the NOAA JPSS data archive on the Amazon Web Services (AWS) via http://noaa-jpss.s3.amazonaws.com/index.html#SNPP/VIIRS/SNPP_VIIRS_Aerosol_Optical_Depth_EDR_Reprocessed/. The data available via AWS is paid for by NOAA and available to the public for free. The Level 2 TROPOMI NO_2 data were downloaded from the European Space Agency datahub (https://s5phub.copernicus.eu/dhus/#/home).

References

Abadie A 2021 Using synthetic controls: feasibility, data requirements, and methodological aspects *J. Econ. Lit.* **59** 391–425

Acharya P, Barik G, Gayen B K, Bar S, Maiti A, Sarkar A, Ghosh S, Kisor S and Sreekesh S 2021 Revisiting the levels of aerosol optical depth in south-southeast Asia, Europe and USA amid the COVID-19 pandemic using satellite observations *Environ. Res.* **193** 110514

Andersen H, Cermak J, Stirnberg R, Fuchs J, Kim M and Pauli E 2021 Assessment of COVID-19 effects on satellite-observed aerosol loading over China with machine learning *Tellus* B **73** 1–13

Andraea M O 2019 Emission of trace gases and aerosols from biomass burning—an updated assessment *Atmos. Chem. Phys.* **19** 8523–46

Asutosh A, Vinoj V, Murukesh N, Ramisetty R and Mittal N 2022 Investigation of June 2020 giant Saharan dust storm using remote sensing observations and model reanalysis *Sci. Rep.* **12** 6114

Cao C *et al* 2021 Mission-long recalibrated science quality suomi NPP VIIRS radiometric dataset using advanced algorithms for time series studies *Remote Sens.* **13** 1075

Cermak J and Knutti R 2009 Beijing olympics as an aerosol field experiment *Geophys. Res. Lett.* **36** L10806

Chan K L, Wiegner M, van Geffen J, De Smedt I, Alberti C, Cheng Z, Ye S and Wenig M 2020 MAX-DOAS measurements of tropospheric NO_2 and HCHO in Munich and the comparison to OMI and TROPOMI satellite observations *Atmos. Meas. Tech.* **13** 4499–520

Ding J, van der A, J. R, Mijling B, Levelt P F and Hao N 2015 NO_x emission estimates during the 2014 youth olympic games in nanjing *Atmos. Chem. Phys.* **15** 9399–412

Gettelman A, Lamboll R, Bardeen C G, Forster P M and Watson-Parris D 2021 Climate impacts of COVID-19 induced emission changes *Geophys. Res. Lett.* **48** e2020GL091805

Gkatzelis G I *et al* 2021 The global impacts of COVID-19 lockdowns on urban air pollution: a review *Elementa* **9** 00176

Guo S, Hu M, Guo Q, Zhang X, Schauer J J and Zhang R 2013 Quantitative evaluation of emission controls on primary and secondary organic aerosol sources during Beijing 2008 Olympics *Atmos. Chem. Phys.* **13** 8303–14

Hammer M S *et al* 2021 Effects of COVID-19 lockdowns on fine particulate matter concentrations *Sci. Adv.* **7** 26

Hao N, Valks P, Loyola D, Cheng Y F and Zimmer W 2011 Space-based measurements of air quality during the world expo 2010 in shanghai *Environ. Res. Lett.* **6** 044004

Huff A, Kondragunta S, Zhang H, Laszlo I, Zhou M, Caicedo V, Delgado R and Levy R 2021 Tracking smoke from a prescribed fire and its impacts on local air quality using temporally resolved GOES-16 ABI aerosol optical depth (AOD) *J. Atmos. Ocean. Technol.* **38** 963–76

Iolango I, Virta H, Eskes H, Hovila J and Douros J 2020 Comparison of TROPOMI/Sentinel 5 Precursor NO_2 observations with ground-based measurements in Helsinki *Atmos. Meas. Tech.* **13** 205–18

Itahashi S, Sakurai T, Shimadera H, Araki S and Hayami H 2021 Long-term trends of satellite-based fine-model aerosol optical depth over the Seto Inland Sea, Japan, over two decades (2001–2020) *Environ. Res. Lett.* **16** 4062

Jones C D *et al* 2021 The climate response to emissions reductions due to COVID-19: initial results from CovidMIP *Geophys. Res. Lett.* **48** e2020GL091883

Judd L M *et al* 2020 Evaluating Sentinel-5P TROPOMI tropospheric NO_2 column densities with airborne and Pandora spectrometers near New York City and Long Island Sound *Atmos. Meas. Tech.* **13** 6113–40

Khan A, Khorat S, Khatun R, Doan Q-V, Nair U S and Niyogi D 2021 Variable Impact of COVID-19 Lockdown on Air Quality across 91 Indian Cities (2021) *Earth Interact.* **25** 57–74

Kondragunta S, Wei Z, McDonald B C, Goldberg D L and Tong D Q 2021 COVID-19 induced fingerprints of a new normal urban air quality in the United States *J. Geophys. Res.* **126** e2021JD034797

Kong L *et al* 2023 Unbalanced emission reductions of different species and sectors in China during COVID-19 lockdown derived by multi-species surface observation assimilation *Atmos. Chem. Phys.* **23** 6217–40

Kroll J H, Heald C L, Cappa C D, Farmer D K, Fry J L, Murphy J G and Steiner A L 2020 The complex chemical effects of COVID-19 shutdowns on air quality *Nat. Chem.* **12** 777–9

Kumar P, Hama S, Omidvarborna H, Sharma A, Sahani J, Abhijith K V, Debele S E, Zavala-Reyes J C, Barwise Y and Tiwari A 2020 Temporary reduction in fine particulate matter due to anthropogenic emissions switch off during COVID-19 lockdown in Indian cities *Sustain. Cities Soc.* **62** 102382

Kumari S, Lakhani A and Kumari K M COVID-19 and air pollution in indian cities: world's most polluted cities 2020 *Special Issue on COVID-19 Aerosol Drivers, Impacts and Mitigation, Aerosol and Air Quality Research* vol 20 pp 2592–603

Laszlo I and Liu H 2016 EPS aerosol optical depth (AOD) theoretical basis document, Version 3.0.1 (available at: www.star.nesdis.noaa.gov/jpss/documents/ATBD/ATBD_EPS_Aerosol_AOD_v3.0.1.pdf) (Accessed 30 May 2022)

Laszlo I 2018 Remote sensing of tropospheric aerosol optical depth from multispectral monodirectional space-based observations *Comprehensive Remote Sensing* ed S Liang (Elsevier) pp 137–96

Le T, Wang Y, Liu L, Yang J, Yung Y L, Li G and Seinfeld J H 2020 Unexpected air pollution with marked emission reductions during the COVID-19 outbreak in China *Science* **369** 702–6

Li K, Jacob D J, Liao H, Shen L, Zhang Q and Bates K 2019 H.: anthropogenic drivers of 2013–2017 trends in summer surface ozone in China *Proc. Natl Acad. Sci. USA* **116** 422–7

Li Y, Tong D, Ma S, Zhang X, Kondragunta S, Li F and Saylor R 2021 Dominance of wildfires impact on air quality exceedances during the 2020 record-breaking wildfire season in the United States *Geophys. Res. Lett.* **48** e2021GL094908

Liu F, Liu M, Lin J, Kong H, Boersma K F and Eskes H 2021 Abrupt decline in tropospheric nitrogen dioxide after the outbreak of COVID-19 *Paper presented at 101st virtual American Meteorological Association Meeting*

Liu H, Remer L A, Huang J, Huang H-C, Kondragunta S, Laszlo I, Oo M and Jackson J M 2014 Preliminary evaluation of S-NPP VIIRS aerosol optical thickness *J. Geophys. Res. Atmos.* **119** 3942–62

Loeb N G, Su W, Bellouin N and Ming Y 2021 Changes in clear-sky shortwave aerosol direct radiative effects since 2002 *J. Geophys. Res.* **126** e2020JD034090

McDuffie E E, Smith S J, O'Rourke P, Tibrewal K, Venkataraman C, Marais E A, Zheng B, Crippa M, Brauer M and Martin R V 2020 A global anthropogenic emission inventory of atmospheric pollutants from sector- and fuel-specific sources (1970–2017): an application of the community emissions data system (CEDS) *Earth Syst. Sci. Data* **12** 3413–42

Mishra M K and Rathore P S 2021 Impact of nationwide COVID-19 lockdown on Indian air quality in terms of aerosols as observed from the space *Aerosol Air Qual. Res.* **21** 200461

Miyazaki K, Bowman K, Sekiya T, Jiang Z, Chen X, Eskes H, Ru M, Zhang Y and Shindell D 2020 Air quality response in China linked to the 2019 novel coronavirus (COVID-19) lockdown *Geophys. Res. Lett.* **47** e2020GL089252

Naeger A R and Murphy K 2020 Impact of COVID-19 containment measures on air pollution in California *Aerosol Air Qual. Res.* **20** 2025–34

Sathe Y, Gupta P, Bawase M, Lamsal L, Patadia F and Thipse S 2021 Surface and satellite observations of air pollution in India during COVID-19 lockdown: implications to air quality *Sustain. Cities Soc.* **66** 102688

Sen P 1968 Estimated of the regression coefficient based on Kendall's Tau *J. Am. Stat. Assoc.* **39** 1379–89

Sogacheva L, Rodriguez E, Kolmonen P, Virtanen T H, Saponaro G, de Leeuw G, Georgoulias A K, Alexandri G, Kourtidis K and van der A R J 2018 Spatial and seasonal variations of aerosols over China from two decades of multi-satellite observations—part 2: AOD time series for 1995–2017 combined from ATSR ADV and MODIS C6.1 and AOD tendency estimations *Atmos. Chem. Phys.* **18** 16631–52

Straka III W, Kondragunta S, Wei Z, Zhang H, Miller S D and Watts A 2021 Examining the Economic and environmental impacts of COVID-19 Using Earth Observation Data *Remote Sens.* **13** 5

Su T, Li Z, Zheng Y, Luan Q and Guo J 2020 Abnormally shallow boundary layer associated with severe air pollution during the COVID-19 lockdown in China *Geophys. Res. Lett.* **47** e2020GL090041

Sun Y *et al* 2016 "APEC Blue": secondary aerosol reductions from emission controls in beijing *Sci. Rep.* **6** 20668

Tan P H, Chou C, Liang J Y, Chou C C K and Shiu C J 2009 Air pollution "holiday effect" resulting from the Chinese new year *Atmos. Environ.* **43** 2114–24

Theil H 1950 A rank-invariant method of linear and polynomial regression analysis. I, II, III *Proc. K. Ned. Akad. Wet.* 53 386–92, 521–5, 1397–412

Tibrewal K and Venkataraman C 2022 COVID-19 lockdown closures of emissions sources in India: lessons for air quality and climate policy *J. Environ. Manage.* **302** 114079

Tong D, Pan L, Chen W, Lamsal L, Lee P, Tang Y, Kim H, Kondragunta S and Stajner I 2016 Impact of the 2008 Global Recession on air quality over the United States: implications for surface ozone levels from changes in NO_x emissions *Geophys. Res. Lett.* **43** 9280–8

Uprety S, Cao C and Shao X 2020 Radiometric consistency between GOES-16 ABI and VIIRS on Suomi NPP and NOAA-20 *J. Appl. Remote Sens.* **14** 032407

van Geffen J, Eskes H J, Boresma K F, Maasakkers J D and Veefkind J P 2019 TROPOMI ATBD of the total and tropospheric NO_2 data products, S5P-KNMI-L2-0005-RP, v1.4.0

Veefkind J P, Boresma K F, Wang J, Kurosu T P, Krotkov N, Chance K and Levelt P F 2011 Global satellite analysis of the relation between and aerosols and short-lived trace gases *Atmos. Chem. Phys.* **11** 1255–67

Venter Z S, Aunan K, Chowdhury S and Lelieveld J 2020 COVID-19 lockdowns cause global air pollution declines *Proc. Natl Acad. Sci.* **117** 18984–90

Wang T *et al* 2010 Air quality during the 2008 Beijing Olympics: secondary pollutants and regional impact *Atmos. Chem. Phys.* **10** 7603–15

Wang Y *et al* 2021 Enhancement of secondary aerosol formation by reduced anthropogenic emissions during Spring Festival 2019 and enlightenment for regional $PM_{2.5}$ control in Beijing *Atmos. Chem. Phys.* **21** 915–26

Wang Y, Zhang F, Li Z, Tan H, Xu H, Ren J, Zhao J, Du W and Sun Y 2017 Enhanced hydrophobicity and volatility of submicron aerosols under severe emission control conditions in Beijing *Atmos. Chem. Phys.* **17** 5239–51

Witte J C, Schoeberl M R, Douglass A R, Gleason J F, Krotkov N A, Gille J C, Pickering K E and Livesey N 2009 Satellite observations of changes in air quality during the 2008 Beijing Olympics and Paralympics *Geophys. Res. Lett.* **36** L17803

Zhang H and Kondragunta S 2021 Daily and hourly surface $PM_{2.5}$ estimation from satellite AOD *Earth Space Sci.* **8** e2020EA001599

Zhang H, Kondragunta S, Laszlo I, Liu H, Remer L A, Huang J, Superczynski S and Ciren P 2016 An enhanced VIIRS aerosol optical thickness (AOT) retrieval algorithm over land using a global surface reflectance ratio database *J. Geophys. Res. Atmos.* **121** 10,717–38

Zhao J *et al* 2017 Insights into aerosol chemistry during the 2015 China Victory Day parade: results from simultaneous measurements at ground level and 260 m in Beijing *Atmos. Chem. Phys.* **17** 3215–32

Zhao X *et al* 2020 Assessment of the quality of TROPOMI high-spatial-resolution NO_2 data products in the greater toronto area *Atmos. Meas. Tech.* **13** 2131–59

Zheng B *et al* 2018 Trends in China's anthropogenic emissions since 2010 as the consequence of clean air actions *Atmos. Chem. Phys.* **18** 14095–111

Zheng H *et al* 2020 Significant changes in the chemical compositions and sources of $PM_{2.5}$ in Wuhan since the city lockdown as COVID-19 *Sci. Total Environ.* **739** 140000

Zhu J, Xia X, Wang J, Zhang J, Wiedinmyer C, Fisher J A and Keller C A 2017 Impact of Southeast Asian smoke on aerosol properties in Southwest China: first comparison of model simulations with satellite and ground observations *J. Geophys. Res. Atmos.* **122** 3904–19

Zhu J, Yue X, Che H, Xia X, Lei Y and Wang J 2022 Contribution of fire emissions to PM2.5 and its transport mechanism over the Yungui Plateau, China during 2015–2019 *J. Geophys. Res.* **127** e2022JD036734